Supplementary Information (SI) for Nanoscale.

Design of MnO_2-based catalysts with activity approaching Pt/C via machine learning

Huang Jiasheng [a], Li Jiangtao [a], Zhu Yuhao [a], Wang Zehao [a], Xu Jian [a], Wang Fu [a], Xia Lan [a], Miao He [a] *, Yuan Jinliang [a]

[a] Faculty of Maritime and Transportation, Ningbo University, Ningbo 315211, PR China

* Corresponding authors:

Prof. He Miao, E-mail: miaohe@nbu.edu.cn

■ **Chemical reagents**

$KMnO_4$ (AR), $Al(NO_3)_3·9H_2O$ (AR), $Cr(NO_3)_3·9H_2O$ (AR), $Fe(NO_3)_3·9H_2O$ (AR), $Co(NO_3)_2·6H_2O$ (AR), $Ni(NO_3)_2·6H_2O$ (AR), $Sr(NO_3)_2·4H_2O$ (AR), $Cd(NO_3)_2·4H_2O$ (AR), $Ce(NO_3)_3·6H_2O$ (AR), $Pr(NO_3)_3·6H_2O$ (AR), $Nd(NO_3)_3·6H_2O$ (AR), $Sm(NO_3)_3·6H_2O$ (AR), $Gd(NO_3)_3·6H_2O$ (AR), KOH (AR), C_2H_5OH (AR), Pt/C, Aluminum foil, Polytetrafluoroethylene preparation (PTFE, 60 wt.%), were purchased from Aladdin Ltd. Conductive carbon (VXC-72) was purchased from Cabot Ltd., and Nafion solution (5 wt%, 80 μL) was obtained from DuPont Ltd. Ni foam was purchased from Sinero Co. Ltd. All chemical reagents in the Experimental section were used directly without the further treatment.

■ **Material characterization**

X-ray diffraction (XRD) patterns were obtained on a Bruker D8 Advance X-ray diffract meter (Cu Kα = 1.5418 Å, Bruker Ltd., Karlsruhe, Germany) at a scanning rate of 0.02° s^{-1} from 10° to 90°. The microstructures and elemental distributions of the synthesized samples were observed using field emission scanning electron microscopy (FESEM, Hitachi S4800, 5 kV, Hitachi Ltd., Tokyo, Japan), transmission electron microscopy (TEM, JF-20, Hitachi), and high-resolution transmission electron microscopy (HRTEM, JF-20, Hitachi).

■ **Preparation of working electrode**

The working electrode was prepared as follows: the catalyst inks were prepared by dispersing 5 mg catalysts and 5 mg carbon (Vulcan-XC72) in 2 mL absolute ethanol, and then 80 μL 5 wt% Nafion solution (DuPont) was added and ultrasonically blended for 1 h to form a well-dispersed ink. 20 μL catalyst ink was carefully dropped onto the glassy carbon electrode (5 mm in diameter) with the catalyst loading of 255 μg cm^{-2}. The working electrodes were then dried in air at room temperature for 1 hour. For comparison, the catalyst of 20 wt% Pt/C (Aladdin Corp.) with the same mass loading were also applied to prepare the working electrode.

■ **Measurement of working electrode**

ORR measurements were conducted in an O_2-saturated 0.1 M KOH solution using a rotating disk electrode (rotation speed fixed at 1600 rpm). Linear sweep voltammetry

(LSV) curves were recorded within a potential range of +0.2 V to –0.8 V (vs. Hg/HgO) at a scan rate of 5 mV s^{-1}. To investigate the reaction pathway during ORR, a rotating ring-disk electrode (RRDE) was employed. A constant potential of 1.4 V (vs. RHE) was applied to the ring electrode to detect hydrogen peroxide generated at the disk electrode. Based on the measured ring current (I_{ring}), disk current (I_{disk}), and the known collection efficiency (N) of the ring, the percentage of hydrogen peroxide intermediate ($X(HO_2^-)$) and the average number of transferred electrons (n_{e^-}) were calculated using the following equations (1) and (2), respectively.

$$n_{e^-} = 4\frac{I_{disk}}{I_{disk} + \frac{I_{ring}}{N}} \quad (1)$$

$$X\left(HO_2^-\right) = 100\frac{2\frac{I_{ring}}{N}}{I_{disk} + \frac{I_{ring}}{N}} \quad (2)$$

The ORR durability of the catalysts was evaluated by chronoamperometry (CA) test in an O_2-saturated 0.1 M KOH solution at a fixed rotation speed of 1600 rpm.

■ **Electrode correction**

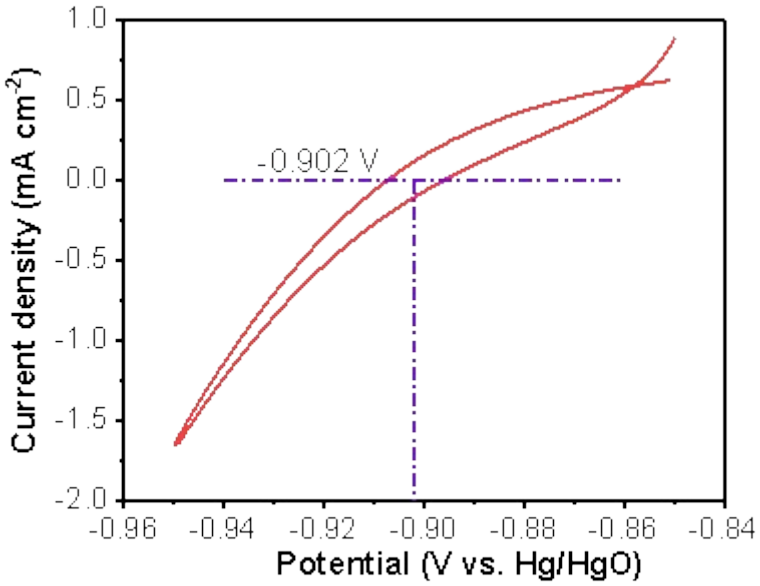

Fig. S1. Cyclic voltammetry curve at a scan rate of 20 mV s^{-1} in H_2-saturated 0.1 M KOH solution for RHE calibration.

The reference electrode was calibrated to a reversible hydrogen electrode (RHE). The RHE calibration was performed in a H_2-saturated 0.1 M KOH solution at 25 ^oC and a Pt tablet with the area of 1 cm^{-2} was used as work electrode. Take the average value of the potential of two curves at zero current as the thermodynamic potential of hydrogen electrode reaction.

In 0.1 M KOH, the reversible hydrogen electrode correction formula of Hg/HgO reference electrode is: E(RHE) = E(Hg/HgO) + 0.902 V.

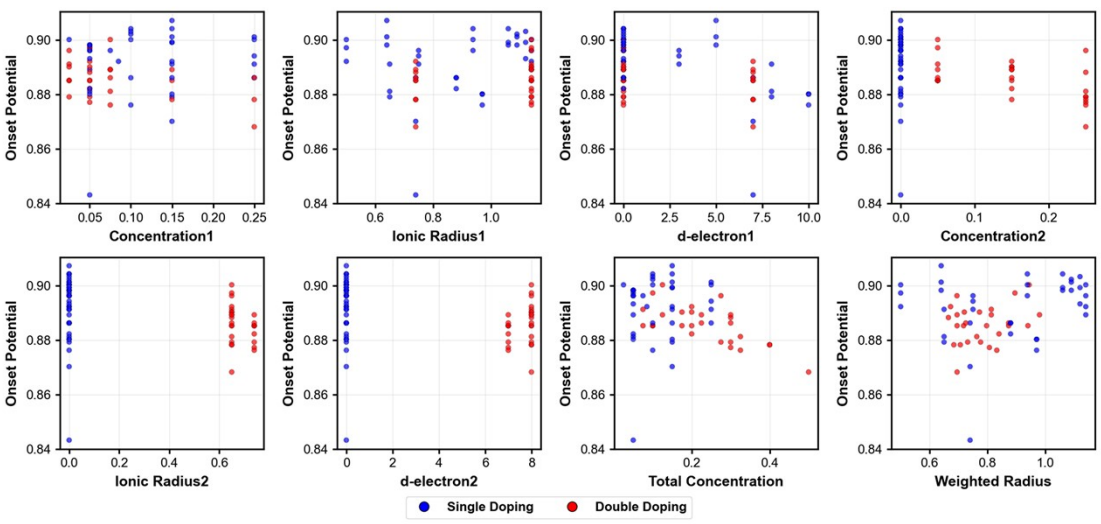

Fig. S2. The distribution plots of characteristic data with respect to onset potentials.

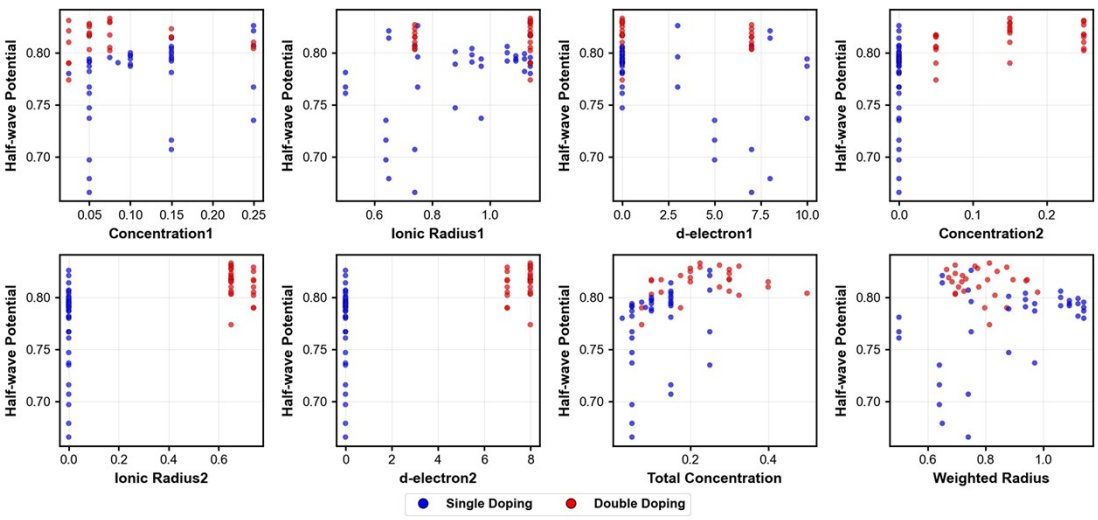

Fig. S3. The distribution plots of characteristic data with respect to half-wave potentials.

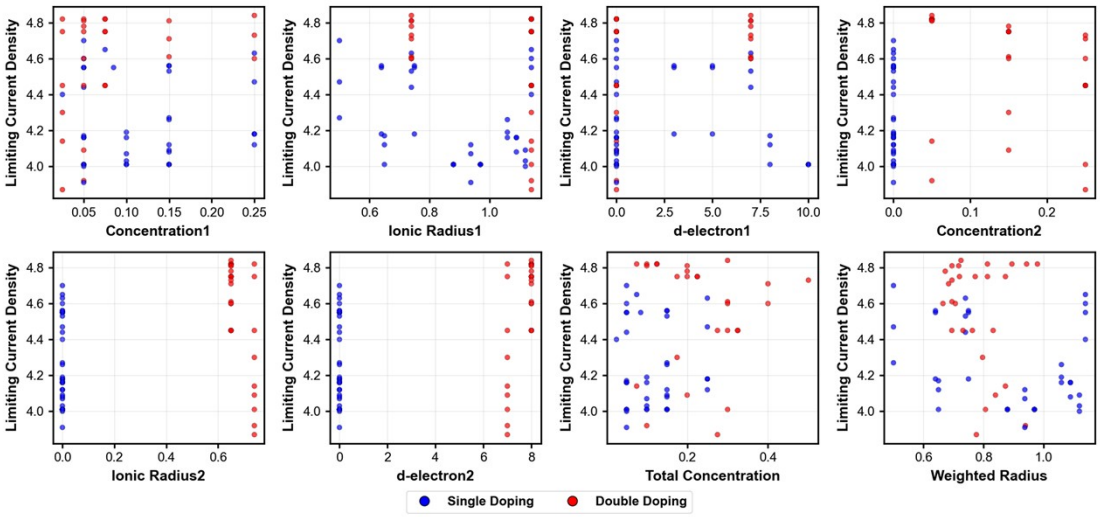

Fig. S4. The distribution plots of characteristic data with respect to limiting current densities.

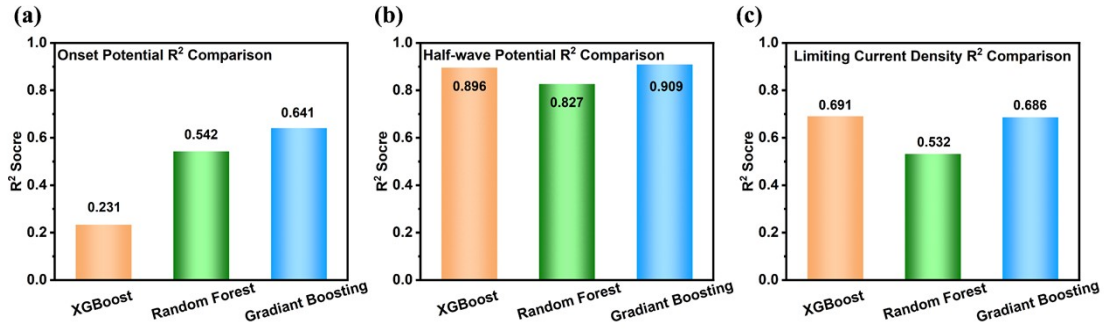

Fig. S5. Average R^2 values of the three models (XGBoost, Random Forest, and Gradient Boosting) obtained from 1000 repeated training runs for the predictions of (a) onset potential, (b) half-wave potential, and (c) limiting current density.

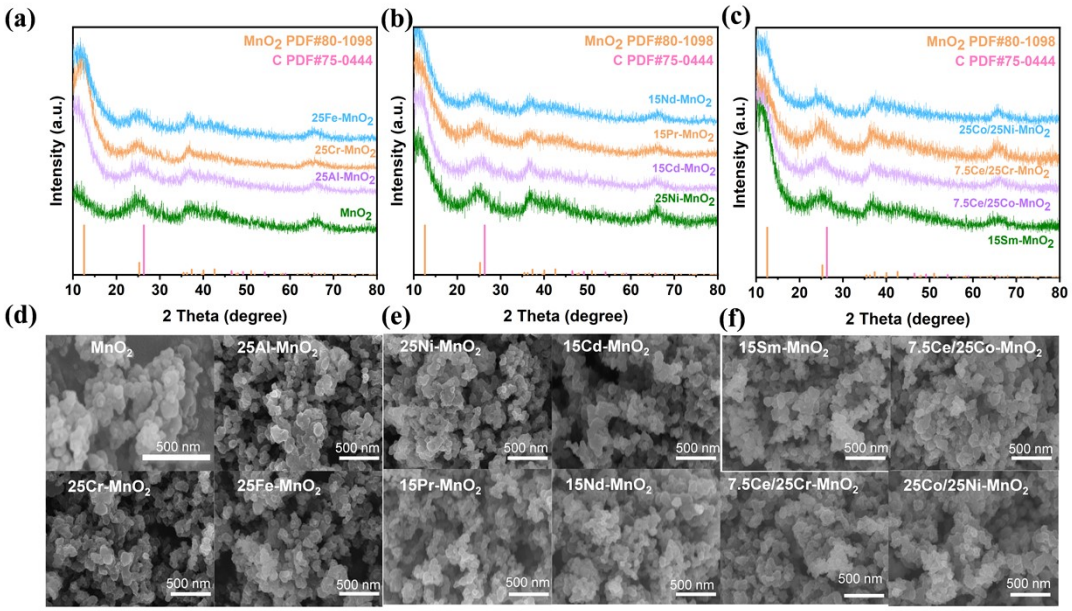

Fig. S6. (a-c) SEM images and (d-f) XRD patterns of δ-MnO_2 with different metal dopants at their maximum concentrations.

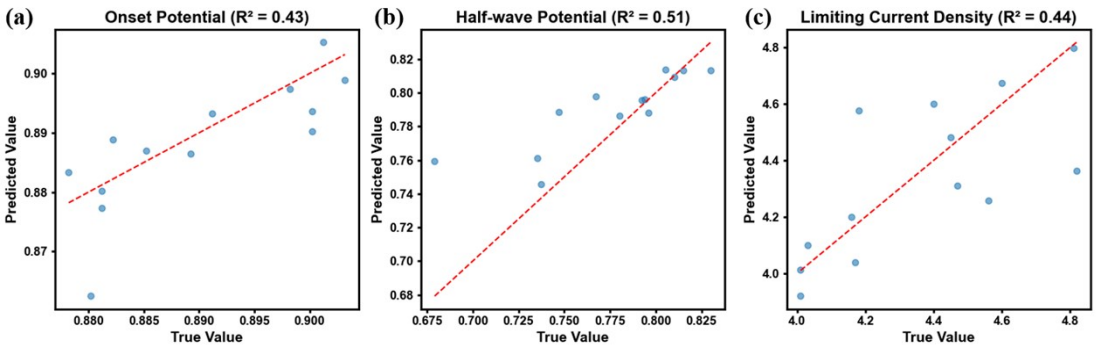

Fig. S7. Effect of removing highly correlated descriptors on model prediction performance (R^2) for (a) E_{onset}, (b) $E_{1/2}$, and (c) J_L.

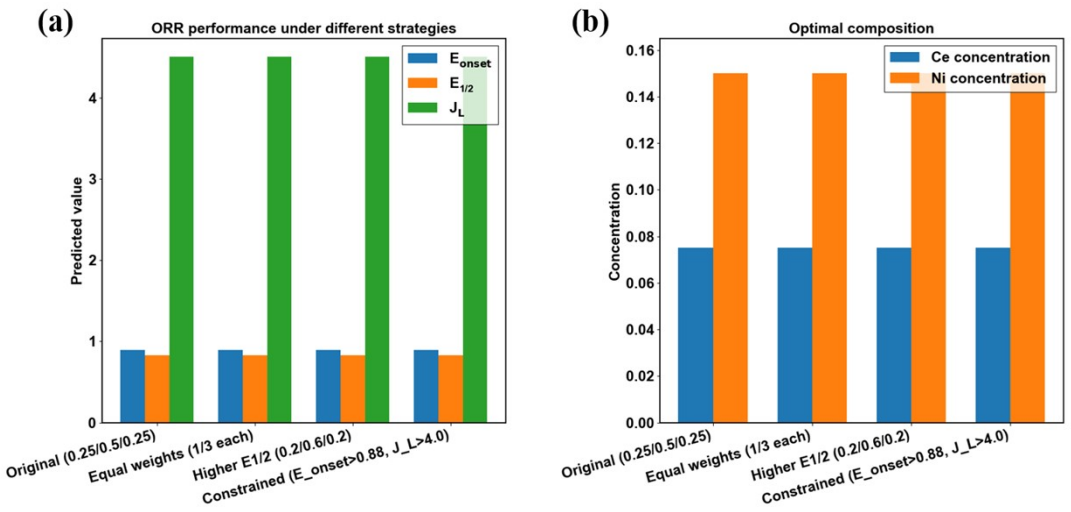

Fig. S8. Sensitivity analysis of the optimal composition under different multi-objective strategies:(a) Predicted ORR performance (E_{onset}, $E_{1/2}$, J_L) for the optimal composition identified under each strategy and (b) Corresponding optimal Ce and Ni concentrations.

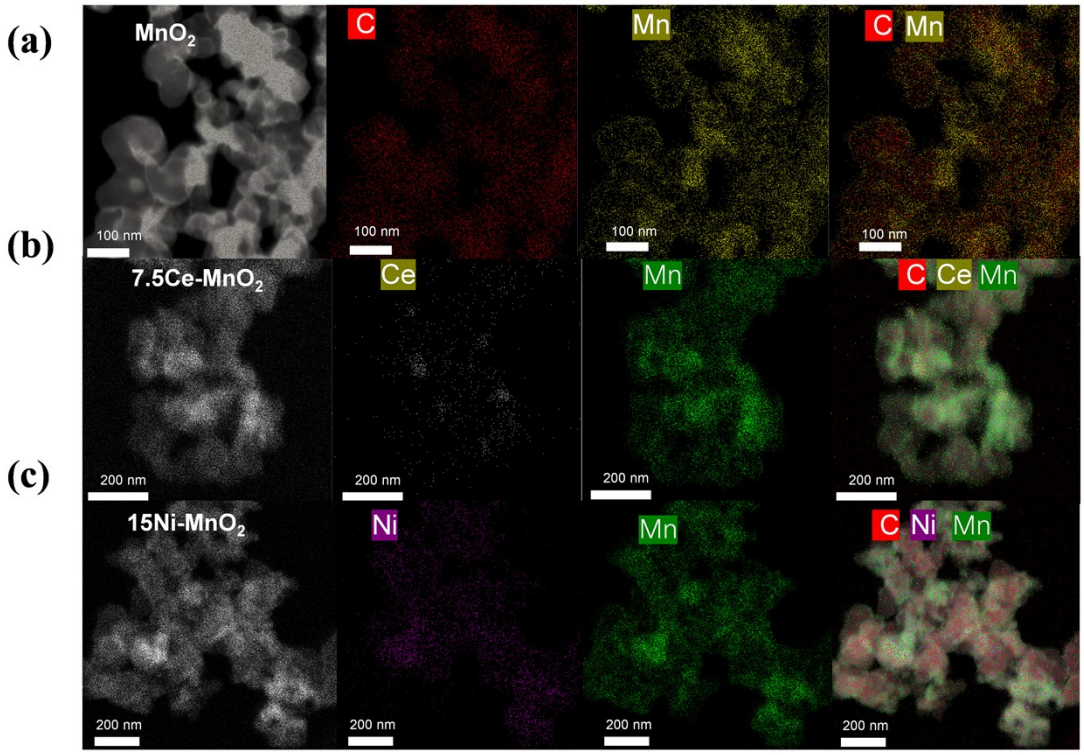

Fig. S9. EDS mappings of (a) MnO_2, (b) 7.5Ce-MnO_2, (c) 15Ni-MnO_2.

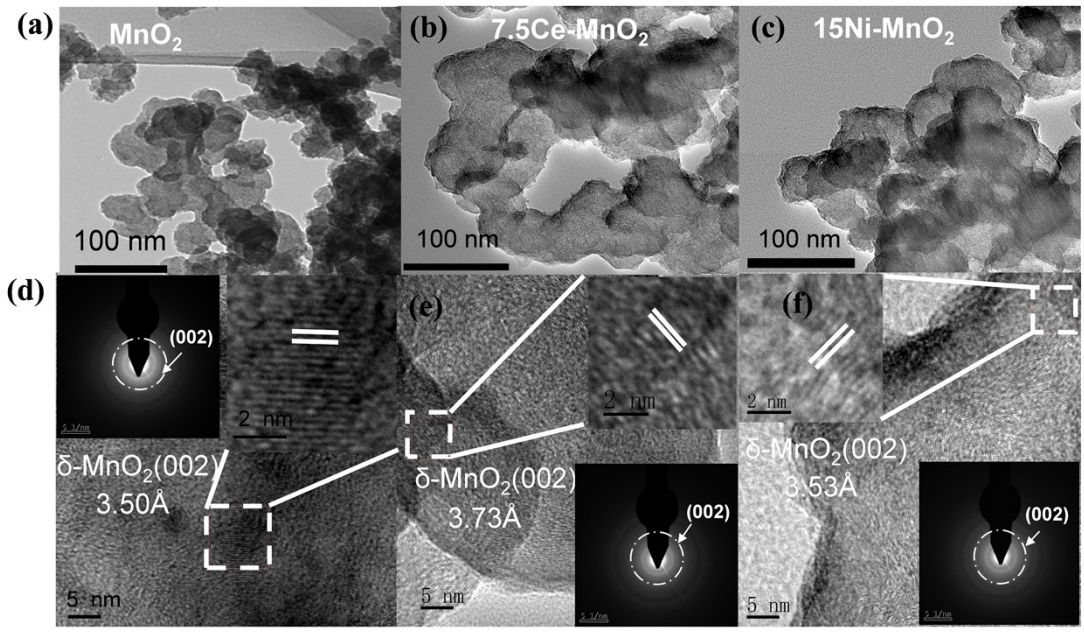

Fig. S10. TEM images of (a) MnO_2, (b) 7.5Ce-MnO_2, and (c) 15Ni-MnO_2. HRTEM images and SAED patterns of (d) MnO_2, (e) 7.5Ce-MnO_2, and (f) 15Ni-MnO_2.

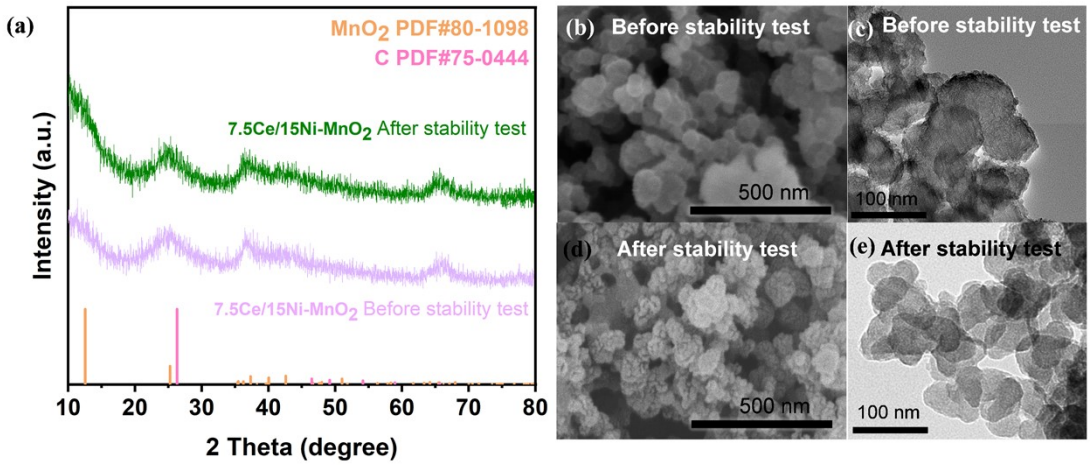

Fig. S11. (a) XRD patterns before and after the stability test. (b, c) SEM and TEM images before the stability test. (d, e) SEM and TEM images after the stability test.

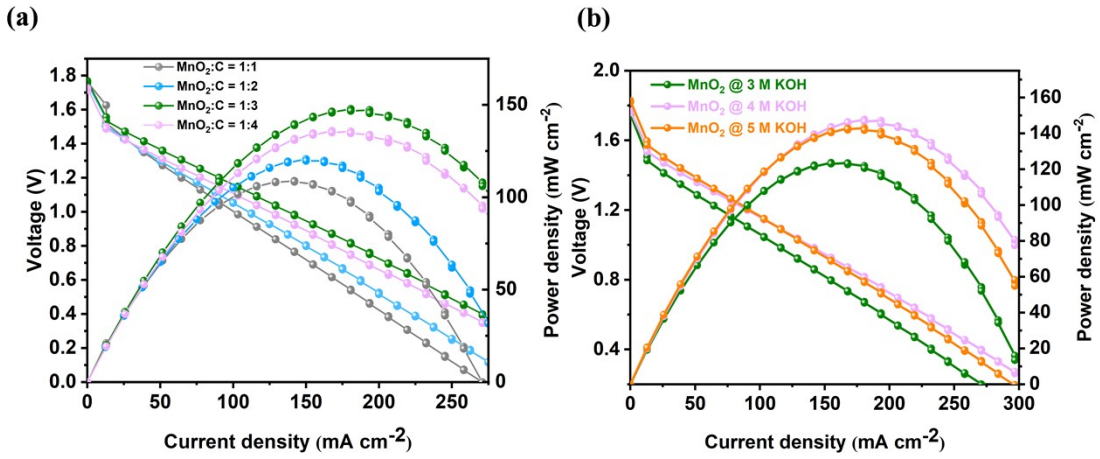

Fig. S12. Discharge polarization curves and corresponding power density curves of Al-air batteries with varying (a) Mn/C ratios and (b) KOH concentrations.

Tab. S1. Comprehensive data table of ORR onset potential, half-wave potential, and limiting current density for all samples.

Sample name	Onset potential (V)	Half-wave potential (V)	limiting current density (mA cm^{-2})
MnO_2	0.8972	0.6782	4.5057
5Al-MnO_2	0.8972	0.7612	4.7000
15Al-MnO_2	0.8922	0.7812	4.2700
25Al-MnO_2	0.9002	0.7672	4.4700
5Fe-MnO_2	0.8982	0.6972	4.5500
15Fe-MnO_2	0.9072	0.7162	4.5600
25Fe-MnO_2	0.9012	0.7352	4.1800
5Co-MnO_2	0.8432	0.6660	4.4400
15Co-MnO_2	0.8702	0.7072	4.5300
25Co-MnO_2	0.8862	0.8072	4.6300
5Ni-MnO_2	0.8812	0.6792	4.1700
15Ni-MnO_2	0.8792	0.8142	4.0100
25Ni-MnO_2	0.8912	0.8082	4.1200
5Cr-MnO_2	0.8962	0.7672	4.5500
15Cr-MnO_2	0.8912	0.7962	4.5600
25Cr-MnO_2	0.8942	0.8132	4.1800
5Cd-MnO_2	0.8962	0.7912	3.9100
15Cd-MnO_2	0.9002	0.7982	4.0700
25Cd-MnO_2	0.9042	0.8042	4.1200
2.5Ce-MnO_2	0.9002	0.7802	4.4000
5Ce-MnO_2	0.8892	0.7872	4.6000
7.5Ce-MnO_2	0.8962	0.7956	4.6500
5Sr-MnO_2	0.8932	0.7822	4.0000
15Sr-MnO_2	0.9032	0.7942	4.0300
25Sr-MnO_2	0.8992	0.7992	4.0900
5Pr-MnO_2	0.8982	0.7942	4.1600

Sample name	Onset potential (V)	Half-wave potential (V)	limiting current density (mA cm^{-2})
10Pr-MnO_2	0.9022	0.7972	4.1600
15Pr-MnO_2	0.9012	0.7922	4.0800
5Nd-MnO_2	0.8982	0.7922	4.1600
10Nd-MnO_2	0.9042	0.8002	4.1900
15Nd-MnO_2	0.8992	0.8062	4.2600
5Sm-MnO_2	0.8802	0.7372	4.0100
10Sm-MnO_2	0.8762	0.7872	4.0100
15Sm-MnO_2	0.8802	0.7942	4.0100
5Gd-MnO_2	0.8822	0.7472	4.0100
10Gd-MnO_2	0.8862	0.7892	4.0100
15Gd-MnO_2	0.8862	0.8012	4.0100
2.5Ce/5Co-MnO_2	0.8852	0.7902	4.1400
2.5Ce/15Co-MnO_2	0.8852	0.7902	4.3000
2.5Ce/25Co-MnO_2	0.8792	0.8102	3.8700
5Ce/5Co-MnO_2	0.8852	0.8162	3.9200
5Ce/15Co-MnO_2	0.8822	0.8202	4.0900
5Ce/25Co-MnO_2	0.8772	0.8172	4.0100
7.5Ce/5Co-MnO_2	0.8892	0.8052	4.8200
7.5Ce/15Co-MnO_2	0.8862	0.8222	4.7500
7.5Ce/25Co-MnO_2	0.8762	0.8022	4.4500
5Co/5Ni-MnO_2	0.8852	0.8032	4.8100
5Co/15Ni-MnO_2	0.8922	0.8192	4.7800
5Co/25Ni-MnO_2	0.8882	0.8180	4.6000
15Co/5Ni-MnO_2	0.8852	0.8152	4.8100
15Co/15Ni-MnO_2	0.8892	0.8202	4.6100
15Co/25Ni-MnO_2	0.8782	0.8152	4.7100
25Co/5Ni-MnO_2	0.8862	0.8062	4.8400
25Co/15Ni-MnO_2	0.8782	0.8102	4.6000

Sample name	Onset potential (V)	Half-wave potential (V)	limiting current density (mA cm^{-2})
25Co/25Ni-MnO_2	0.8682	0.8042	4.7300
2.5Ce/5Cr-MnO_2	0.8912	0.7740	4.8200
2.5Ce/15Cr-MnO_2	0.8902	0.8212	4.7500
2.5Ce/25Cr-MnO_2	0.8962	0.8222	4.4500
5Ce/5Cr-MnO_2	0.8972	0.8172	4.8200
5Ce/15Cr-MnO_2	0.8902	0.8232	4.7500
5Ce/25Cr-MnO_2	0.8792	0.8180	4.4500
7.5Ce/5Cr-MnO_2	0.9002	0.8172	4.8200
7.5Ce/15Cr-MnO_2	0.8892	0.8232	4.7500
7.5Ce/25Cr-MnO_2	0.8812	0.8222	4.4500

Tab. S2. Variance inflation factor (VIF) values for the features.

Feature	VIF	Feature	VIF
Concentration 1	12527.52	Δr1-Mn	72.316536
Ion Radius 1	13637.31	Δr2-Mn	inf
d-Electron 1	15380.59	Total Conc.	inf
Concentration 2	inf	Conc. Ratio	33.69
Ion Radius 2	inf	Conc. Product	11.35
d-Electron 2	inf	Radius Diff.	inf
r1 vs Mn	inf	Weighted Radius	11727.11
r2 vs Mn	inf		